CHIN. PHYS. LETT. Vol. 37, No. 3 (2020) 038503

High-Performance Germanium Waveguide Photodetectors on Silicon *

Xiu-Li Li(李秀丽)[1,2], Zhi Liu(刘智)[1,2**], Lin-Zhi Peng(彭林志)[1,2], Xiang-Quan Liu(刘香全)[1,2], Nan Wang(王楠)[1,2], Yue Zhao(赵越)[1,2], Jun Zheng(郑军)[1,2], Yu-Hua Zuo(左玉华)[1,2], Chun-Lai Xue(薛春来)[1,2], Bu-Wen Cheng(成步文)[1,2]

[1]*State Key Laboratory on Integrated Optoelectronics, Institute of Semiconductors, Chinese Academy of Sciences, Beijing 100083*

[2]*Center of Materials Science and Optoelectronics Engineering, University of Chinese Academy of Sciences, Beijing 100049*

(Received 26 November 2019)

Germanium waveguide photodetectors with 4 μm widths and various lengths are fabricated on silicon-on-insulator substrates by selective epitaxial growth. The dependence of the germanium layer length on the responsivity and bandwidth of the photodetectors is studied. The optimal length of the germanium layer to achieve high bandwidth is found to be approximately 8 μm. For the 4 × 8 μm² photodetector, the dark current density is as low as 5 mA/cm² at −1 V. At a bias of −1 V, the 1550 nm optical responsivity is as high as 0.82 A/W. Bandwidth as high as 29 GHz is obtained at −4 V. Clear opened eye diagrams at 50 Gbits/s are demonstrated at 1550 nm.

PACS: 85.60.Gz, 42.82.Et, 42.79.Sz DOI: 10.1088/0256-307X/37/3/038503

To meet the demands of optical interconnect systems and fast-growing data communications exceeding 100 Gbits/s, low-cost, low-power, and high-speed optical components must be developed. Si photonics is a promising technology to satisfy these requirements.[1,2] Germanium waveguide photodetectors on Si substrates are key Si photonic devices owing to their compatibility with the typical CMOS process and the relatively high absorption coefficient of germanium in the near-infrared region.[3] In recent years, germanium waveguide photodetectors on Si have been developed by many researchers.[4–9] The −3 dB bandwidth, optical responsivity, and dark current density are critical parameters for the high performance of germanium waveguide photodetectors. However, these parameters are interdependent, and tradeoffs between them must be found. It is generally known that the waveguide photodetectors can be divided into lateral and vertical PIN junction structures. Researchers have improved the −3 dB bandwidth to 67 GHz using a lateral positive-intrinsic-negative (PIN) structure. However, this reduced the responsivity to 0.74 A/W at 1550 nm and required the precise control of the etching process.[8] Using a vertical PIN structure with a larger germanium layer area ($4.4 \times 100\ \mu m^2$) achieved an optical responsivity of 1.16 A/W and the fabrication process was simple, but a decrease was observed in the bandwidth with increasing germanium layer's area due to the increased resistor-capacitor (RC) delay.[10] Researchers increased the −3 dB bandwidth to 45 GHz using a small germanium layer ($1.3 \times 4\ \mu m^2$), whereas this degraded the responsivity and the dark current density was as large as 57 mA/cm². In addition, a complex fabrication process, such as chemical-mechanical polish, was required.[5] Therefore, further research is required on the tradeoff between the responsivity and bandwidth of germanium photodetectors with various germanium layers and on the reduction of the dark current of the devices.

In this study, we fabricate germanium waveguide photodetectors with germanium layer's lengths of 6, 8, and 12 μm on silicon-on-insulator (SOI) substrates. The dependences of the responsivity and bandwidth on the germanium layer's length are analyzed. The length of the germanium layer is optimized to guarantee the overall good performance in terms of bandwidth and responsivity. The dark current and eye diagram characteristics are investigated to find the noise and signal transmission characteristics of the devices.

The germanium waveguide photodetectors were fabricated in a commercial foundry. A schematic cross-sectional view of the photodetector is shown in Fig. 1(a). The devices were installed on an SOI substrate with a 220-nm-thick Si top layer and a 2-μm-thick buried oxide layer. The 220 nm silicon layer was etched to define the grating coupler, Si waveguide, and photodetectors. A 500-nm-thick germanium layer was selectively grown on the n-type top silicon layer, which was implanted with phosphorous to form the n-type contact layer. Three germanium layers were grown separately with widths of 4 μm and lengths of 6, 8, and 12 μm. The top of the germanium layer was implanted with boron to form the p-type contact layer. Contact holes and metal to p-type germanium/n-type silicon were fabricated. Finally, the pad contact holes were fabricated to connect the test probe. Figures 1(b)–

*Supported by the National Key Research and Development Program of China (Grant No. 2017YFA0206404), the National Natural Science Foundation of China (Grant Nos. 61435013, 61534005, 61534004, 61604146, and 61774143), the Key Research Program of Frontier Sciences, CAS (Grant No. QYZDY-SSW-JSC022), and the Beijing Education Commission Project (Grant No. SQKM201610005008).

**Corresponding author. Email: zhiliu@semi.ac.cn

1(d) show the micrograph of the photodetector with pads, 3D structure diagram of the germanium waveguide photodetectors, and size of the photodetectors, respectively.

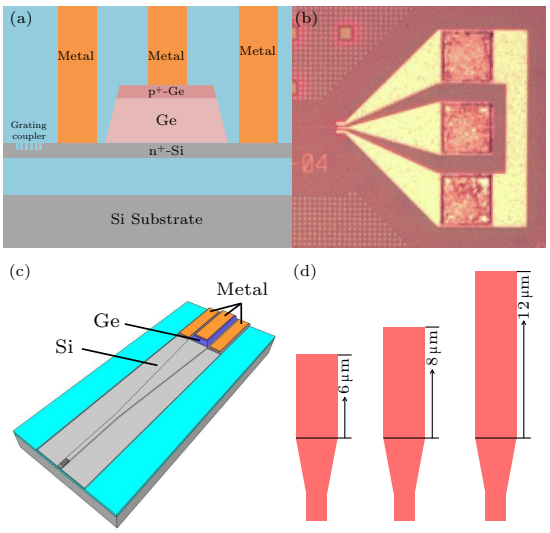

Fig. 1. (a) Schematic cross-sectional view of the photodetector. (b) Micrograph of the photodetector with pads. (c) Three-dimensional structure diagram of the germanium photodetectors. (d) Size of the devices.

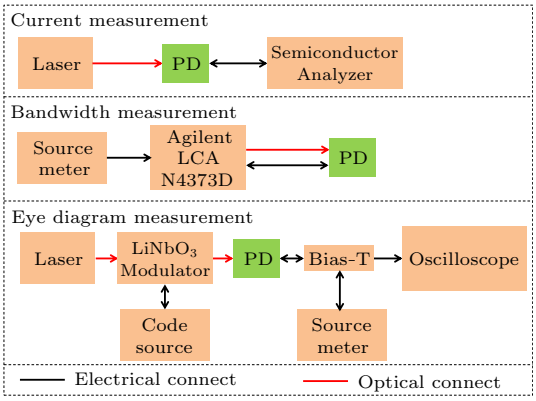

Fig. 2. Schematic of the experimental setup for the measurements of the dark current, photocurrent, bandwidth, and eye diagram. The red and black lines represent the optical and electrical connections, respectively. PD: photodetector.

Figure 2 shows flow charts of the experimental setup for the measurements of the dark current, photocurrent, bandwidth, and eye diagram. The red and black lines represent the optical and electrical connections, respectively.

The I–V characteristics of the photodetectors with and without incident light were measured using an Agilent B1500A semiconductor parameter analyzer, a probe station, and a Santec tunable semiconductor laser (TSL-550) at room temperature. The incident light was introduced to the grating coupler by a single-mode tapered lensed fiber. The optical power output from the tapered lensed fiber was measured by a calibrated commercial reference detector.

High-frequency characteristics of the photodetectors were measured using the Agilent 67 GHz lightwave-component-analyzer (LCA) N4373D in the test range from 10 MHz to 40 GHz with a radio-frequency GSG probe of 65 GHz (50 Ω load resistance). The modulated output light at 1550 nm from the integrated Agilent LCA system was transmitted through optical fibers, and an optical polarizer was used to maximize the incident light power into the photodetectors. The bias voltage from the Keithley 2611A system source meter was applied to the photodetectors through the integrated Agilent LCA system via the radio-frequency GSG probe.

The eye diagrams were measured on the wafer. A $(2^{31}-1)$ long optical nonreturn-to-zero (NRZ) pseudo-random bit sequence data pattern with various data rates generated by a commercial $LiNbO_3$ modulator at 1550 nm was delivered to the grating coupler of the photodetectors. The upper limit of the $LiNbO_3$ modulator operation range was 50 Gbits/s. A sampling oscilloscope was used to observe the eye diagrams.

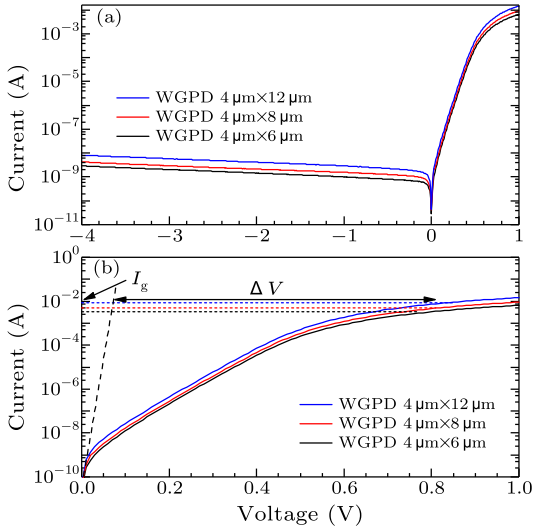

Fig. 3. (a) I–V characteristics of the germanium photodetectors with dark currents. (b) Extracted series resistance (R_{pd}) from the forward I–V characteristics.

One of the most critical characteristics of high-performance germanium waveguide photodetectors is the dark current. Low dark currents can reduce the noise of photodetectors, which is very important for high signal-to-noise ratios (SNRs) of optical receivers. Figure 3(a) displays the I–V curves of the photodetectors with various sizes at bias voltages from −4 V to 1 V. At the bias voltage of −1 V, the dark currents in the photodetectors with sizes of 4×6, 4×8, and 4×12 μm^2 are 1.0, 1.5, and 2.9 nA, respectively. These values are considered to be acceptable for high-speed optical receivers.[11] The dark current density is approximately 5 mA/cm^2, which is due to the superior quality of the germanium layer and the accurate device fabrication process. In addition, an on/off current ratio above 5×10^6 is realized between 1 and −1 V, which indicates the excellent PIN junction characteristics. The I–V relationship of the photodetectors can be expressed as $I = I_0[\exp(qV/nkT) - 1]$, where I_0

is the reverse saturated current, k is the Boltzmann constant, T is the temperature, and n is the ideality factors. By taking the logarithm of both sides, the relationship $\ln I = \ln I_0 + qV/nkT$ is obtained. It can be seen that there is a linear relationship between $\ln I$ and V, the ratio coefficient is q/nkT, and the ideality factors n can be obtained by fitting the linear part of the $\ln I$–V curve. The ideality factor of the photodetectors is approximately 1.23, which indicates that the currents of devices are limited by both the diffusion current and generation-recombination current mechanisms.[12]

In a quasi-neutral region, the forward I–V characteristics are mainly affected by the series resistance ($R_{\rm pd}$) of the device.[12] As shown in Fig. 3(b), the $R_{\rm pd}$ can be extracted from the forward I–V characteristics by linear fitting under the logarithmic current coordinates. The voltage drop by comparing the experimental curve to the ideal curve of the device at a given current is obtained at a given current, and the series resistance is calculated by the equation[13]

$$R_{\rm pd} = \frac{\Delta V}{I_{\rm g}}, \tag{1}$$

where $I_{\rm g} = 7.72\times10^{-3}$, 5.86×10^{-3}, and 3.98×10^{-3} A for the devices with sizes of 4×12, 4×8, and $4\times6\,\mu{\rm m}^2$, respectively, corresponding to ΔV of 0.75, 0.69, and 0.64 V. Therefore, the series resistances ($R_{\rm pd}$) of the devices are 96, 117, and 161 Ω, respectively. It can be seen that the $R_{\rm pd}$ increases gradually as the size of the device decreases. This is because the series resistance of the device includes the junction resistance and contact resistance. For shorter devices, the PIN junction area and contact area of the device are smaller, which all result in a larger series resistance of the device.

Normally, the responsivity of germanium waveguide photodetectors increases as the length of the germanium layer increases. Figure 4(a) presents the I–V curves with incident 1550 nm light, and the inset shows a schematic of the optical coupling. The coupling angle between the tapered fiber and the grating coupler is 10°. Under this condition, the coupling loss at 1550 nm is approximately 10 dB. The optical power from the tapered fiber is 0 dBm. Accordingly, the optical power incident onto the photodetector is approximately −10 dBm. At 0 V, the photocurrents of the photodetectors with germanium layer's lengths of 6, 8, and 12 μm are 79, 88, and 95 μA, respectively.

The optical responsivity R can be calculated using the equation $R = (I_{\rm light} - I_{\rm dark})/P$, where $I_{\rm light}$ is the photocurrent, $I_{\rm dark}$ is the dark current, and P is the optical power. The optical responsivities of the devices are displayed in Fig. 4(b). At a bias of 0 V, the optical responsivities of the photodetectors with the germanium layer's lengths of 6, 8, and 12 μm are 0.79, 0.88, and 0.95 A/W, respectively. For the analysis of the dependence of the responsivity on the length of the germanium layer, the FDTD software is used to calculate the responsivity and external quantum efficiency of the photodetectors with various germanium layer lengths.[14,15] The responsivity of the photodetectors simulated by the FDTD software is shown in Fig. 4(b), where the solid-blue line represents the simulation results. The simulated results are higher than the experimental data, which is attributed to the light absorbed by the 100-nm-thick p^+-germanium layer, where the photo-carriers are difficult to be extracted by the electric field. According to the simulation results, more than 93% of the 1550 nm light will be absorbed by the 12-μm-long device, which implies that the responsivity of the device will tend to increase slightly and saturate with longer devices.

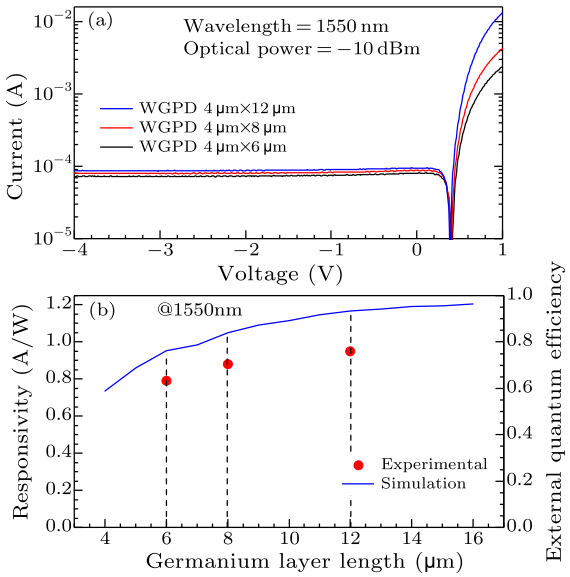

Fig. 4. (a) I–V curves with 1550 nm light. The inset shows a schematic of the optical coupling between the tapered fiber and the grating coupler. (b) Experimental and simulation results of the 1550 nm optical responsivity.

Furthermore, for the $4\times8\,\mu{\rm m}^2$ photodetector, the 1550 nm optical responsivities are 0.883, 0.824, 0.803, 0.790, and 0.787 A/W at biases of 0, −1, −2, −3, and −4 V, respectively. It can be seen that the optical responsivity decreases gradually as the bias voltage increases, which is attributed to the Franz–Keldysh effect.[16,17] This phenomenon is observed in all of the photodetectors.

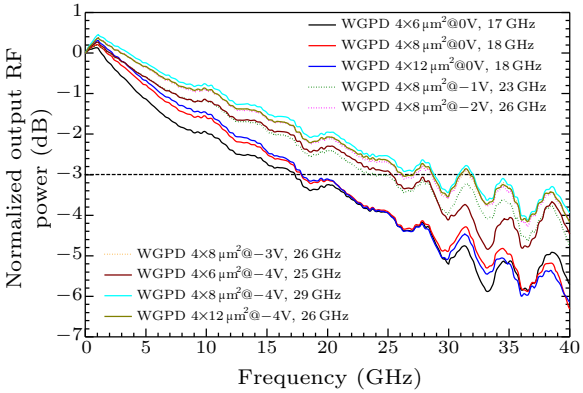

Fig. 5. Normalized frequency responses of the photodetectors with germanium layers of different lengths.

Increasing the length of the germanium layer in the photodetectors will increase not only the light absorption but also the junction capacitance, resulting in lower frequency response. The normalized frequency responses of the photodetectors with different germanium layer's lengths are shown in Fig. 5. At zero bias, the −3 dB bandwidths of the devices with germanium layer's lengths of 6, 8, and 12 μm are 17, 18, and 18 GHz, respectively, which gradually increase as the reverse bias voltage increases. At a bias voltage of −4 V, the −3 dB bandwidths of the devices with germanium layer's lengths of 6, 8, and 12 μm are 25, 29, and 26 GHz, respectively.

The theoretical calculation of the bandwidth enables us to understand and analyze the high-speed performance of the devices further. It is known that the bandwidth of a germanium photodetector is mainly dominated by the carrier transit-time-limited bandwidth f_{T} and RC-limited bandwidth f_{RC} in the active region.[18] The carrier transit-time-limited bandwidth (f_{T}) can be written as[19]

$$f_{\mathrm{T}} = \frac{0.45v}{d}, \tag{2}$$

where v is the saturation drift velocity (Ge: $v = 6 \times 10^6$ cm/s), and d is the thickness of the intrinsic layer. Therefore, the carrier transit-time-limited bandwidth f_{T} is estimated to be approximately 67.5 GHz.

The RC-limited bandwidth f_{RC} can be written as

$$f_{\mathrm{RC}} = \frac{1}{2\pi RC}, \tag{3}$$

where R is the resistance, which consists of the series resistance R_{pd} and the load resistance R_{load}, and C is the capacitance, including the junction capacitance C_{j} and the parasitic capacitance C_{p}. The junction capacitance C_{j} can be calculated by $C_{\mathrm{j}} = \varepsilon\varepsilon_0 WL/d$, where ε and ε_0 are the relative and vacuum permittivity, respectively, W and L are the width and length of the photodetector, respectively, and d is the thickness of the intrinsic layer. The series resistance R_{pd} is extracted from the forward I–V characteristics. The load resistance R_{load} and parasitic capacitance C_{p} are 50 Ω and 17 fF in our test equipment, respectively. Then, the RC bandwidth (f_{RC}) of the photodetectors with different germanium layer's lengths can be calculated. The RC parameters and bandwidths considered are summarized in Table 1.

Table 1. Resistor–capacitor (RC) parameters and bandwidths.

Size (μm^2)	R_{pd} (Ω)	R_{load} (Ω)	C_{j} (fF)	C_{p} (fF)	f_{RC} (GHz)	f_{T} (GHz)	$f_{-3\mathrm{dB}}^{\mathrm{theory}}$ (GHz)	$f_{-3\mathrm{dB}}^{\mathrm{experiment}}$@−4 V (GHz)
4 × 6	161	50	8.6	17	28.7	67.5	27	25
4 × 8	117	50	11.5	17	35.3	67.5	30	29
4 × 12	96	50	17.3	17	31.8	67.5	28.8	26

The −3 dB bandwidth, determined by both carrier transit-time-limited bandwidth f_{T} and RC limited bandwidth f_{RC}, can be estimated by[19]

$$f_{-3\mathrm{dB}} = \frac{1}{\sqrt{f_{\mathrm{T}}^{-2} + f_{\mathrm{RC}}^{-2}}}. \tag{4}$$

The theoretical results obtained for the devices with germanium layer's lengths of 6, 8, and 12 μm are 27, 30, and 28.8 GHz, which are consistent with the experimental data. The photodetector with a germanium layer's length of 8 μm exhibits higher bandwidth than those with germanium layer's lengths of 6 and 12 μm. This is because the bandwidth of the 6-μm-long germanium layer photodetector is mainly limited by the larger series resistance R_{pd}, and that of the 12-μm-long germanium layer photodetector is mainly limited by the larger junction capacitance C_{j}. Therefore, for high-speed germanium waveguide photodetectors on Si, the length of the germanium layer on the device can neither be too long nor too short.

The 50 Gbits/s eye diagrams of the photodetectors at 0, −1, −2, and −3 V are shown in Fig. 6. The photocurrent of the devices is approximately 150 μA. The integration time of the eye diagram is approximately 40 s. Under a bias of 0 V, the eye diagrams are somewhat weak, which is attributed to the relatively low −3 dB bandwidth. When the reverse bias voltage reaches −1 V, all the devices show excellent opened eye diagrams, indicating a high-quality data reception performance.

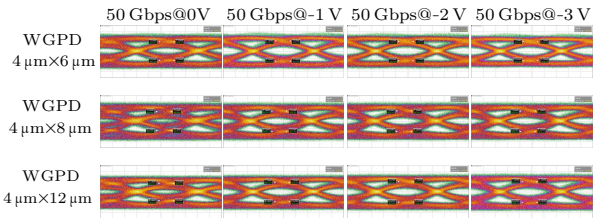

Fig. 6. The 50 Gbits/s eye diagrams of the germanium photodetectors at biases of 0, −1, −2, and −3 V.

In summary, although the optical responsivity of the photodetectors increases with the length of the germanium layer, the bandwidth of the photodetectors with longer germanium layers is limited by the larger junction capacitance C_{j}. Therefore, the length of the germanium layer should not be too long for high-performance waveguide photodetectors. At the same time, the bandwidth of the device with shorter germanium layers is limited by the larger series resistance R_{pd}, so the germanium length should not be too short either. Among the germanium layer's lengths considered in this study, the optimal one for high-performance waveguide photodetectors is 8 μm. For the 4 × 8 μm^2 photodetector, at a bias of −1 V,

the dark current density is approximately 5 mA/cm^2 and the 1550 nm optical responsivity is as high as 0.82 A/W. The −3 dB bandwidth is as high as 29 GHz at −4 V. Clear opened eye diagrams are obtained at 50 Gbits/s.

References

[1] Won R and Paniccia M 2010 *Nat. Photon.* **4** 498
[2] Marpaung D, Yao J and Capmany J 2019 *Nat. Photon.* **13** 80
[3] Michel J, Liu J and Kimerling L C 2010 *Nat. Photon.* **4** 527
[4] Vivien L, Osmond J, Fedeli J M, Marris-Morini D, Crozat P, Damlencourt J F, Cassan E, Lecunff Y and Laval S 2009 *Opt. Express* **17** 6252
[5] DeRose C T, Trotter D C, Zortman W A, Starbuck A L, Fisher M, Watts M R and Davids P S 2011 *Opt. Express* **19** 24897
[6] Liao S, Feng N N, Feng D, Dong P, Shafiiha R, Kung C C, Liang H, Qian W, Liu Y, Fong J, Cunningham J E, Luo Y and Asghari M 2011 *Opt. Express* **19** 10967
[7] Vivien L, Polzer A, Marris-Morini D, Osmond J, Hartmann J M, Crozat P, Cassan E, Kopp C, Zimmermann H and Fedeli J M 2012 *Opt. Express* **20** 1096
[8] Chen H, Verheyen P, De Heyn P, Lepage G, De Coster J, Balakrishnan S, Absil P, Yao W, Shen L, Roelkens G and Van Campenhout J 2016 *Opt. Express* **24** 4622
[9] Cui J and Zhou Z 2017 *Opt. Lett.* **42** 5141
[10] Yin T, Cohen R, Morse M M, Sarid G, Chetrit Y, Rubin D and Paniccia M J 2007 *Opt. Express* **15** 13965
[11] Ahn D, Hong C Y, Liu J, Giziewicz W, Beals M, Kimerling L C, Michel J, Chen J and Kartner F X 2007 *Opt. Express* **15** 3916
[12] Sze S M and Ng K K 2006 *Physics of Semiconductor Devices* (Berlin: Wiley-Interscience)
[13] Liu H X, Wu X F, Hu S G and Shi L C 2010 *Chin. Phys. B* **19** 057303
[14] Goyal P and Kaur G 2018 *Arab. J. Sci. Eng.* **43** 415
[15] Nunley T N, Fernando N S, Samarasingha N, Moya J M, Nelson C M, Medina A A and Zollner S 2016 *J. Vac. Sci. & Technol. B* **34** 061205
[16] Li Y M , Hu W X , Cheng B W , Liu Z and Wang Q M 2012 *Chin. Phys. Lett.* **29** 034205
[17] Schmid M, Kaschel M, Gollhofer M, Oehme M, Werner J, Kasper E and Schulze J 2012 *Thin Solid Films* **525** 110
[18] Liu Z, Yang F, Wu W, Cong H, Zheng J, Li C, Xue C, Cheng B and Wang Q 2017 *J. Lightwave Technol.* **35** 5306
[19] Oehme M, Werner J, Kasper E, Jutzi M and Berroth M 2006 *Appl. Phys. Lett.* **89** 071117